Journal of Solid Mechanics Vol. 9, No. 3 (2017) pp. 663-679

Time-Dependent Hygro-Thermal Creep Analysis of Pressurized FGM Rotating Thick Cylindrical Shells Subjected to Uniform Magnetic Field

A. Bakhshizadeh[1], M. Zamani Nejad [1,*], M. Davoudi Kashkoli [2]

[1]*Department of Mechanical Engineering, Yasouj University, Yasouj, Iran*
[2]*Department of Mechanical Engineering, Shahid Chamran University of Ahvaz, Ahvaz, Iran*

Received 29 June 2017; accepted 30 August 2017

ABSTRACT

Time-dependent creep analysis is presented for the calculation of stresses and displacements of axisymmetric thick-walled cylindrical pressure vessels made of functionally graded material (FGM). For the purpose of time-dependent stress analysis in an FGM pressure vessel, material creep behavior and the solutions of the stresses at a time equal to zero (i.e. the initial stress state) are needed. This corresponds to the solution of the problem considering linear elastic behavior of the material. Therefore, using equations of equilibrium, stress–strain and strain–displacement, a differential equation for displacement is obtained and subsequently the initial elastic stresses at a time equal to zero are calculated. Assuming that the Magneto-hygro-thermoelastic creep response of the material is governed by Norton's law, using the rate form of constitutive differential equation, the displacement rate is obtained and then the stress rates are calculated. Once the stress rates are known, the stresses at any time are calculated iteratively. The analytical solution is obtained for the plane strain condition. The pressure, inner radius and outer radius are considered to be constant and the magnetic field is uniform. Material properties are considered as power law function of the radius of the cylinder and the poisson's ratio as constant. Following this, profiles are plotted for different values of material exponent for the radial, circumferential and effective stresses as a function of radial direction and time. The in-homogeneity exponent have significant influence on the distributions of the creep stresses.

Keywords: Thick cylindrical pressure vessel; Magneto-hygro-thermoelastic-creep; Time-dependent; Functionally graded material (FGM).

1 INTRODUCTION

FUNCTIOALLY graded materials (FGMs) are microscopically inhomogeneous composite materials, in which the material properties vary smoothly and continuously from one surface to the other (Xie, Dai & Rao [1]). The main advantage is that the mechanical properties vary continuously across the shell thickness, which eliminates stress discontinuities typical of composite laminates. Today, FGMs find engineering applications in aerospace structures, chemical and mechanical industries, etc (Levyakov & Kuznetsov [2]). Several studies have

*Corresponding author. Tel.: +98 7431005000; Fax: +98 7431005000.
E-mail address: m_zamani@yu.ac.ir (M. Zamani Nejad).

been performed by researchers on the static behavior of FGM structures (Nejad & Fatehi [3], Nejad, Jabbari & Ghannad [4-5-6], Nejad, Rastgoo & Hadi [7]).

Thick shells involving cylindrical pressure vessels, in recent years, are widely used in space vehicles, aircrafts, nuclear power plants and many other engineering application (Nejad, Jabbari, & Ghannad [8-9], Jabbari, Nejad & Ghannad [10-11]). Elastic, plastic and creep stress analysis of these components has attracted wide attention due to the combination of different material properties and loading conditions. Creep stresses in FGM thick cylindrical shells under thermal loading have been analyzed extensively with regard to the elastic material behavior in the past years. Attia, Fitzgeorge and Pope [12] investigated the residual stresses produced in cast iron cylinder by the creep-relaxation of thermal stresses. In this study a series of thick-hollow cylinders are subjected to a radial flow of heat by heating the bore and water-cooling the outer diameter for a chosen period of time, during which the thermal stresses are relaxed by creep. Weir [13] investigated creep stresses in pressurized thick walled tubes. Assuming the simply supported and fixed-end boundary conditions for the cylinders, Wah [14] developed a theory for the collapse of cylindrical shells under steady-state creep and under external radial pressure and high temperature (300 to 500 *F*.). Bhatnagar and Gupta [15] obtained solution for an orthotropic thick-walled internally pressurized cylinder by using constitutive equations of anisotropy creep and Norton's creep law. Besseling [16] investigated the feasibility of a numerical analysis of nonstationary creep problems for thick-walled tubes under axially symmetric loading. Pai [17] studied the steady-state creep of a thick-walled orthotropic cylinder subjected to internal pressure. They observed that the creep anisotropy has a significant effect on the cylinder behavior particularly in terms of creep rates which may differ by an order of magnitude compared to an isotropic analysis. Sankaranarayanan [18] studied the steady creep behavior of thin circular cylindrical shells subjected to combined lateral and axial pressures. The analysis is based on the Tresca criterion and the associated flow rule. Assuming that the total strain is consist of elastic and creep components, Murakami and Iwatsuki [19] investigated the transient creep analysis of circular cylindrical shells on the basis of the strain-hardening and time-hardening theories. Murakami and Suzuki [20] developed a numerical analysis of the steady state creep of a pressurized circular cylindrical shell on the basis of Mises' criterion and the power law of creep. Sim and Penny [21] studied the deformation behavior of thick-walled tubes subjected to a variety of loadings during stress redistribution caused by creep. Murakami and Iwatsuki [22] investigated the steady state creep of simply supported circular cylindrical shells with open ends under internal pressure by using Nortons's law. Kashkoli and Nejad [23] investigated the effect of heat flux on creep stresses of thick-walled cylindrical pressure vessels by using Nortons's law. Using finite-strain theory Bhatnagar and Arya [24] studied the creep behavior of a thick-walled cylinder under large strains. Murakami and Tanaka [25] investigated the creep buckling of clamped circular cylindrical shells subjected to axial compression combined with internal pressure with special emphasis on the concept of creep stability and the accuracy of the analysis. Jones and Sullivan [26] studied the advantages and limitations of a perturbation method of analysis for the creep buckling of shells by examining the particular case of a long cylindrical shell subjected to a uniform external pressure. Arya, Debnath and Bhatnagar [27] investigated the problem of creep in a thin circular cylindrical shell made of a homogeneous, incompressible and orthotropic material using a non-steady creep law. Creep damage simulation of thick-walled tubes using the theta projection concept was investigated by Loghman and Wahab [28]. They obtained a closed-form solution for steady state creep stresses in FGM cylinders. Yang [29] presented an analytical solution for the calculation of stresses in FGM for the elastic and creep behavior of the materials. This solution can be used to study the dependence of stress on temperature and time for FG structures. Finally, the analytical results were compared with FEM. Gupta and Pathak [30], studied thermo creep analysis in a pressurized thick hollow cylinder. Jahed and Bidabadi [31] presented a general axisymmetric method for an inhomogeneous body for a disk with varying thickness. An approximation has been employed during their solution algorithm. It means that they avoid considering the differentiation constitutive terms of governing equations for creep analysis. Chen, Tu, Xuan and Wang [32] studied the creep behavior of a functionally graded cylinder under both internal and external pressures. They observed that an asymptotic solution can be derived on the basis of a Taylor series expansion if the properties of the graded material are axisymmetric and dependent on radial coordinate. In order to investigate creep performance of thick-walled cylindrical vessels or cylinders made of functionally graded materials, You, Ou and Zheng [33] proposed a simple and accurate method to determine stresses and creep strain rates in thick-walled cylindrical vessels subjected to internal pressure. Based on the power law constitutive equation, Altenbach, Gorash and Naumenko [34] presented the classical solution of the steady-state creep problem for a pressurized thick-walled cylinder. In this paper they applied an extended constitutive equation which includes both the linear and the power law stress dependencies. Singh and Gupta [35-36-37-38] developed a mathematical model to describe the steady-creep behavior of functionally graded composite cylinders containing linearly varying silicon carbide particles in a matrix of pure aluminum involving threshold stress-based creep law. The model developed is used to investigate the effect of gradient in distribution of SiCp on the steady-state creep response of the composite cylinder. Nejad and

Kashkoli [39] investigated time-dependent thermo-elastic creep response for isotropic rotating thick-walled cylindrical pressure vessels made of FGM, taking into account the creep behavior of the pressure vessels, as described in Norton's model.

Assuming total strains to be the sum of elastic, thermal and creep strains, Loghman, Arani, Amir and Vajedi [40] studied the time-dependent creep stress redistribution analysis of a thick-walled FGM cylinder placed in uniform magnetic and temperature fields and subjected to an internal pressure. Following Norton's law for material creep behavior and using equations of equilibrium, strain displacement and stress-strain relations in the rate form and considering Prandtl-Reuss relations for creep strain rate-stress equation, they obtained a differential equation for the displacement rate and then calculated the radial and circumferential creep stress rates. Singh and Gupta [41] investigated the steady state creep in transversely isotropic functionally graded cylinder, operating under internal and external pressures. In this paper the effect of anisotropy on creep stresses and creep rates in the FGM cylinder has been analyzed and compared with an isotropic FGM cylinder. Assuming that the thermo-elastic creep response of the material is governed by Norton's law, Kashkoli and Nejad [42] presented an analytical solution for the calculation of stresses and displacements of FGM thick-walled spherical pressure vessels. Dai and Zheng [43] presented the creep buckling and post-buckling analyses of the viscoelastic FGM cylindrical shell with initial deflection subjected to a uniform in plane load by adopting the Boltzmann linear superposition principle. Sharma, Sahay and Kumar [44] investigated the creep stresses in thick-walled circular cylinders under internal and external pressure, using transition theory, which is based on the concept of 'generalized principal strain measure'. Jamian, Sato, Tsukamoto and Watanabe [45] investigated the creep analysis for a thick-walled cylinder made of functionally graded materials (FGMs) subjected to thermal and internal pressure. Singh and Gupta [46] studied the steady state creep behavior in a functionally graded thick composite cylinder subjected to internal pressure in the presence of residual stress. Hoffman's yield criterion is used, to describe the yielding of the cylinder material in order to account for residual stress. Assuming plane strain condition, Nejad, Hoseini, Niknejad and Ghannad [47] presented an exact solution for the analysis of FGM rotating thick cylindrical pressure vessels subjected to a steady state creep condition. Norton's power law of creep is employed to derive general expressions for stresses and strain rates. Kashkoli, Tahan and Nejad [48-49] presented a theoretical solution for time-dependent thermo-elastic creep analysis of functionally graded (FG) and homogeneous thick-walled cylinders based on the first-order shear deformation theory. Sharma, Yadav and Sharma [50] investigated the creep behavior of a functionally graded cylinder in torsion under internal and external pressure which is subjected to thermal loading. Loghman, Shayestemoghadam and Loghman [51] studied the creep behavior of strains, stresses, and displacement rates in a thick-walled cylinder made of polypropylene reinforced by functionally graded (FG) multi-walled carbon nanotubes (MWCNTs) using Burgers viscoelastic creep model. Loghman and Atabakhshian [52] studied the time-dependent creep behavior of rotating cylinders made from exponentially graded material using Bailey-Norton creep constitutive model. The results show that using exponentially graded material significantly decreases creep strains, stresses and deformations of the EGM rotating cylinder. Ghorbanpour Arani, Kolahchi, Mosallaie Barzoki and Loghman [53] studied the history of stresses, deformation and electric potential of a thick hollow FGM rotating cylinder made of radially polarized anisotropic piezoelectric material, (e.g., PZT-7A), using a semi-analytical method base on Mendelson's method of successive elastic solution. Aleayoub and Loghman [54] investigated the time-dependent creep stress redistribution analysis of thick-walled FGM spheres subjected to an internal pressure and a uniform temperature field. The results show that radial stress redistributions are not significant for different material properties. However, major redistributions occur for tangential and effective stresses.

In this article, assuming that the Magneto-hygro-thermoelastic-creep response of the material is governed by Norton's law, an analytical solution is presented for the calculation of stresses and displacements of FGM thick-walled cylindrical pressure vessels. The governing coupled differential equations are exactly solved. The cylinder is subjected to internal and external pressure and uniform magnetic field. The temperature and moisture concentration distributions are obtained separately in an uncoupled hygro-thermal analysis by solving heat conduction and moisture diffusion equations.

2 GEOMETRY , LOADING CONDITION, MATERIAL PROPERTIES AND CREEP CONSTITUTIVE MODEL

A thick-walled, cylindrical vessel made of functionally graded material with an inner radius a and outer radius b with perfect conductivity is considered. Let the cylindrical coordinates of any representative point be (r,θ,z) and

assume that the cylinder subjected to a radially changing of temperature $T(r)$ and moisture concentration $M(r)$. The cylinder is placed in a uniform magnetic field $\vec{H}=(0,0,H_z)$ and subjected to internal pressure P_i and external pressure P_0, and also an inertia body force due to the rotation of the cylindrical vessel with a constant angular velocity of ω. The material properties are assumed to be radially dependent, In this study, Poisson's ratio, *v*, is considered to be a constant and modulus of elasticity, *E*, density, ρ, thermal expansion coefficient, α, moisture concentration coefficient, β, thermal conductivity, k^T, moisture diffusivity coefficient, k^M and magnetic permeability, μ, are assumed to obey the power-law variation as:

$$E=E_0\left(\frac{r}{b}\right)^{\gamma_1} \tag{1}$$

$$\alpha=\alpha_0\left(\frac{r}{b}\right)^{\gamma_2} \tag{2}$$

$$\beta=\beta_o\left(\frac{r}{b}\right)^{\gamma_3} \tag{3}$$

$$k^T=k_0{}^T\left(\frac{r}{b}\right)^{\gamma_4} \tag{4}$$

$$k^M=k_0{}^M\left(\frac{r}{b}\right)^{\gamma_5} \tag{5}$$

$$\rho=\rho_o\left(\frac{r}{b}\right)^{\gamma_6} \tag{6}$$

$$\mu=\mu_0\left(\frac{r}{b}\right)^{\gamma_7} \tag{7}$$

Here γ_i is the in-homogeneity constants determined empirically. The uniaxial creep constitutive model is the Norton's law,

$$\dot{\varepsilon}_e^c=B(r)\sigma_e^{n(r)} \tag{8}$$

where *r* is the radial coordinate, $\dot{\varepsilon}_e^c$ and σ_e are effective stress and effective strain, respectively and $B(r)$ and $n(r)$ are the radial-dependent material creep parameters as:

$$B(r)=b_0 r^{b_1} \tag{9}$$

$$n(r)=n_0 \tag{10}$$

where b_0, b_1 and n_0 are material constants for creep.

3 HEAT CONDUCTION AND MOISTURE DIFFUSION FORMULATION

In the steady state case, the heat conduction equation for the one-dimensional problem in polar coordinates simplifies to,

$$\frac{1}{r}\frac{\partial}{\partial r}\left(rk^{T}\frac{\partial T}{\partial r}\right)=0 \tag{11}$$

where k^{T} is the thermal conductivity. It is to be noted that the thermal conductivity k^{T} is also changed through the radial direction of the cylinder according to Eq. (6). We may determine the temperature distribution in the cylindrical vessel by solving Eq. (11) and applying appropriate boundary conditions. Eq. (11) may be integrated twice to obtain the general solution,

$$T\left(r\right)=W_{1}r^{-\gamma_{4}}+W_{2} \tag{12}$$

The boundary conditions for temperature are,

$$\begin{cases}T=T_{i} & , \quad r=a\\ T=T_{o} & , \quad r=b\end{cases} \tag{13}$$

Applying these conditions to the general solution, we then obtain,

$$\begin{cases}W_{1}=\dfrac{T_{i}-T_{o}}{a^{-\gamma_{4}}-b^{-\gamma_{4}}}\\ W_{2}=\dfrac{T_{o}a^{-\gamma_{4}}-T_{i}b^{-\gamma_{4}}}{a^{-\gamma_{4}}-b^{-\gamma_{4}}}\end{cases} \tag{14}$$

In modeling, the transient moisture diffusion equation is analogous to the transient heat conduction equation. It can be described by the following equation,

$$\frac{1}{r}\frac{\partial}{\partial r}\left(rk^{M}\frac{\partial M}{\partial r}\right)=0 \tag{15}$$

where the moisture diffusivity coefficient k^{M} is also changed across the thickness of the cylinder according to Eq. (7). The general solution of the moisture diffusion equation is,

$$M\left(r\right)=S_{1}r^{-\gamma_{5}}+S_{2} \tag{16}$$

The boundary conditions for the moisture concentration are,

$$\begin{cases}M=M_{i} & , \quad r=a\\ M=M_{o} & , \quad r=b\end{cases} \tag{17}$$

Applying these conditions to the general solution, we then obtain,

$$\begin{cases}S_{1}=\dfrac{M_{i}-M_{o}}{a^{-\gamma_{5}}-b^{-\gamma_{5}}}\\ S_{2}=\dfrac{M_{o}a^{-\gamma_{5}}-M_{i}b^{-\gamma_{5}}}{a^{-\gamma_{5}}-b^{-\gamma_{5}}}\end{cases} \tag{18}$$

4 FORMULATION OF THE MAGNETO-HYGRO-THERMOELASTIC CREEP ANALYSIS

4.1 Solution for linear elastic behavior of FGM thick cylindrical pressure vessel

For the stress analysis in an FGM thick cylindrical pressure vessel, having material creep behavior, the solutions of the stresses at a time equal to zero (i.e. the initial stress state) are needed. This corresponds to the solution of materials with linear elastic behavior. Assuming total strains to be the sum of elastic, thermal, moisture and creep strains then the stress-strain relation for axisymmetric plane strain condition in cylindrical coordinate may be written in terms of radial displacement as:

$$\sigma_r = c_{11}\frac{\partial u}{\partial r} + c_{12}\frac{u}{r} - \lambda_1 T - \zeta_1 M - \lambda_2 \varepsilon_r^c \tag{19}$$

$$\sigma_\theta = c_{12}\frac{\partial u}{\partial r} + c_{11}\frac{u}{r} - \lambda_1^{/} T - \zeta_1^{/} M - \lambda_2 \varepsilon_\theta^c \tag{20}$$

where σ_r and σ_θ are radial and circumferential stresses, respectively, u is radial displacement and ε_r^c and ε_θ^c are radial and circumferential creep strains, respectively. Also,

$$\lambda_1 = c_{11}\alpha_r + c_{12}\left(\alpha_z + \alpha_\theta\right) \tag{21}$$

$$\lambda_1^{/} = c_{11}\alpha_\theta + c_{12}\left(\alpha_z + \alpha_r\right) \tag{22}$$

$$\lambda_2 = \frac{E}{(1+\nu)} \tag{23}$$

$$\zeta_1^{/} = c_{11}\beta_\vartheta + c_{12}\left(\beta_z + \beta_r\right) \tag{24}$$

$$\zeta_1^{/} = c_{11}\beta_\vartheta + c_{12}\left(\beta_z + \beta_r\right) \tag{25}$$

Considering $\alpha_r = \alpha_z = \alpha_\vartheta = \alpha$ and $\beta_r = \beta_z = \beta_\vartheta = \beta$ then,

$$c_{11} = \frac{E(1-\nu)}{(1+\nu)(1-2\nu)} \tag{26}$$

$$c_{12} = \frac{E\nu}{(1+\nu)(1-2\nu)} \tag{27}$$

$$\lambda_1 = \lambda_1^{/} = \frac{E\alpha}{(1-2\nu)} \tag{28}$$

$$\lambda_2 = \frac{E}{(1+\nu)} \tag{29}$$

$$\zeta_1 = \zeta_1^{/} = \frac{E\beta}{(1-2\nu)} \tag{30}$$

The equation of the stress equilibrium inside the FGM cylindrical pressure vessel is,

$$\frac{\partial \sigma_r}{\partial r}+\frac{\sigma_r-\sigma_\vartheta}{r}+F_z=-\rho r\omega^2 \tag{31}$$

where F_z is the Lorentz's force which can be written in terms of radial displacement as:

$$F_z=\mu(r)H_z^2\frac{\partial}{\partial r}\left(\frac{\partial}{\partial r}+\frac{u}{r}\right) \tag{32}$$

Substituting Eqs.(19),(20) and (32) into equilibrium Eq.(31), and assuming that ($\gamma_i=\gamma$; $i=1,2,...,7$) the following differential equation for displacement is obtained,

$$\begin{aligned} &r^2\frac{d^2u}{dr^2}+(I\gamma+1)r\frac{du}{dr}+(L\gamma-1)u=\left(\frac{1+\nu}{1-\nu}\right)I\left(\frac{r}{b}\right)^\gamma\left[2\gamma\alpha_0Tr+\alpha_0r^2\frac{dT}{dr}+2\gamma\beta_0Mr+\beta_0r^2\frac{dM}{dr}\right]\\ &+\left(\frac{1-2\nu}{1-\nu}\right)I\left[\gamma r\varepsilon_r^c+r^2\frac{d\varepsilon_r^c}{dr}+r\left(\varepsilon_r^c-\varepsilon_\theta^c\right)\right]-\frac{\rho r^3\omega^2(1+\nu)(1-2\nu)}{E_0(1-\nu)+\mu_0H_z^2(1+\nu)(1-2\nu)} \end{aligned} \tag{33}$$

where,

$$I=\frac{E_0(1-\nu)}{E_0(1-\nu)+\mu_0H_z^2(1+\nu)(1-2\nu)} \tag{34}$$

$$L=\frac{\nu}{1-\nu}I \tag{35}$$

Ignoring the creep strains in Eq. (33) and considering a uniform temperature field T and a uniform moisture field M the following differential equation for magnetothermoelastic analysis is obtained,

$$\begin{aligned} &r^2\frac{d^2u}{dr^2}+(I\gamma+1)r\frac{du}{dr}+(L\gamma-1)u=(\frac{1+\nu}{1-\nu})I\left(\frac{r}{b}\right)^\gamma\left[2\gamma\alpha_0Tr+\alpha_0r^2\frac{dT}{dr}+2\gamma\beta_0Mr+\beta_0r^2\frac{dM}{dr}\right]\\ &-\frac{\rho r^3\omega^2(1+\nu)(1-2\nu)}{E_0(1-\nu)+\mu_0H_z^2(1+\nu)(1-2\nu)} \end{aligned} \tag{36}$$

The general solution of the displacement u is,

$$u(r)=u_c+u_p=C_1r^{m_1}+C_2r^{m_2}+G_1r^3+G_2r^{\gamma+3}+G_3r^5 \tag{37}$$

where,

$$\begin{aligned} &m_{1,2}=-\frac{\gamma\pm\sqrt{I^2\gamma^2-4L\gamma+4}}{2}\quad,\quad G_1=\left(\frac{1+\nu}{1-\nu}\right)\frac{\gamma I\left(\alpha_0W_1+\beta_0S_1\right)}{b^\gamma(3-m_1)(3-m_2)}\\ &G_2=2\left(\frac{1+\nu}{1-\nu}\right)\frac{\gamma I\left(\alpha_0W_1+\beta_0S_1\right)}{b^\gamma(3-m_1+\gamma)(3-m_2+\gamma)}\quad,\quad G_3=-\frac{\rho\omega^2(1-2\nu)(1+\nu)}{\left[E_0(1-\nu)+\mu_0H_z^2(1+\nu)(1-2\nu)\right](5-m_1)(5-m_2)} \end{aligned} \tag{38}$$

The corresponding stresses are,

$$\sigma_r = (\bar{c}_{11}m_1 + \bar{c}_{12})C_1 r^{\gamma+m_1-1} + (\bar{c}_{11}m_2 + \bar{c}_{12})C_2 r^{\gamma+m_2-1} + (3\bar{c}_{11} + \bar{c}_{12})G_1 r^{\gamma+2} + ((\gamma+3)\bar{c}_{11} + \bar{c}_{12})G_2 r^{2\gamma+2} + (5\bar{c}_{11} + \bar{c}_{12})G_3 r^{\gamma+4} - (\bar{\lambda}_1 W_1 + \bar{\zeta}_1 S_1)r^{\gamma} - (\bar{\lambda}_1 W_2 + \bar{\zeta}_1 S_2)r^{2\gamma} \quad (39)$$

$$\sigma_\theta = (\bar{c}_{12}m_1 + \bar{c}_{11})C_1 r^{\gamma+m_1-1} + (\bar{c}_{12}m_2 + \bar{c}_{11})C_2 r^{\gamma+m_2-1} + (3\bar{c}_{12} + \bar{c}_{11})G_1 r^{\gamma+2} + ((\gamma+3)\bar{c}_{12} + \bar{c}_{11})G_2 r^{2\gamma+2} + (5\bar{c}_{12} + \bar{c}_{11})G_3 r^{\gamma+4} - (\bar{\lambda}_1 W_1 + \bar{\zeta}_1 S_1)r^{\gamma} - (\bar{\lambda}_1 W_2 + \bar{\zeta}_1 S_2)r^{2\gamma} \quad (40)$$

To determine the unknown constants C_1 and C_2 in each material, boundary conditions have to be used, which are,

$$\begin{cases} \sigma_r = -P_i & , \quad r = a \\ \sigma_r = -P_o & , \quad r = b \end{cases} \quad (41)$$

These constants are written as follows,

$$C_1 = \Big\{\big(P_o a^{\gamma+m_2-1} - P_i b^{\gamma+m_2-1}\big) + (3\bar{c}_{11} + \bar{c}_{12})G_1\big[a^{\gamma+m_2-1}b^{\gamma+2} - a^{\gamma+2}b^{\gamma+m_2-1}\big] + \big((\gamma+3)\bar{c}_{11} + \bar{c}_{12}\big)G_2\big[a^{\gamma+m_2-1}b^{2\gamma+2} - a^{2\gamma+2}b^{\gamma+m_2-1}\big] + (5\bar{c}_{11} + \bar{c}_{12})G_3\big[a^{\gamma+m_2-1}b^{\gamma+4} - a^{\gamma+4}b^{\gamma+m_2-1}\big] + \big(\bar{\lambda}_1 W_1 + \bar{\zeta}_1 S_1\big)\big(a^{\gamma}b^{\gamma+m_2-1} - a^{\gamma+m_2-1}b^{\gamma}\big) + \big(\bar{\lambda}_1 W_2 + \bar{\zeta}_1 S_2\big)\big(a^{2\gamma}b^{\gamma+m_2-1} - a^{\gamma+m_2-1}b^{2\gamma}\big)\Big\} \Big/ \Big\{(\bar{c}_{11}m_1 + \bar{c}_{12})\big(a^{\gamma+m_1-1}b^{\gamma+m_2-1} - a^{\gamma+m_2-1}b^{\gamma+m_1-1}\big)\Big\} \quad (42)$$

$$C_2 = \Big\{\big(P_o a^{\gamma+m_1-1} - P_i b^{\gamma+m_1-1}\big) + (3\bar{c}_{11} + \bar{c}_{12})G_1\big[a^{\gamma+m_1-1}b^{\gamma+2} - a^{\gamma+2}b^{\gamma+m_1-1}\big] + \big((\gamma+3)\bar{c}_{11} + \bar{c}_{12}\big)G_2\big[a^{\gamma+m_1-1}b^{2\gamma+2} - a^{2\gamma+2}b^{\gamma+m_1-1}\big] + (5\bar{c}_{11} + \bar{c}_{12})G_3\big[a^{\gamma+m_1-1}b^{\gamma+4} - a^{\gamma+4}b^{\gamma+m_1-1}\big] + \big(\bar{\lambda}_1 W_1 + \bar{\zeta}_1 S_1\big)\big(a^{\gamma}b^{\gamma+m_1-1} - a^{\gamma+m_1-1}b^{\gamma}\big) + \big(\bar{\lambda}_1 W_2 + \bar{\zeta}_1 S_2\big)\big(a^{2\gamma}b^{\gamma+m_1-1} - a^{\gamma+m_1-1}b^{2\gamma}\big)\Big\} \Big/ \Big\{(\bar{c}_{11}m_2 + \bar{c}_{12})\big(a^{\gamma+m_2-1}b^{\gamma+m_1-1} - a^{\gamma+m_1-1}b^{\gamma+m_2-1}\big)\Big\} \quad (43)$$

4.2 Solution for creep behavior of FGM thick cylindrical pressure vessel

Considering the temperature and moisture fields to be steady the differential Eq. (33) containing creep strains may be rewritten in terms of creep strain rates as follows:

$$r^2\frac{d^2\dot{u}}{dr^2} + (I\gamma+1)r\frac{d\dot{u}}{dr} + (L\gamma-1)\dot{u} = \left(\frac{1-2\nu}{1-\nu}\right)I\left[\gamma r\dot{\varepsilon}_r^c + r^2\frac{d\dot{\varepsilon}_r^c}{dr} + r\left(\dot{\varepsilon}_r^c - \dot{\varepsilon}_\theta^c\right)\right] \quad (44)$$

Creep strain rates are related to the stresses and the material uniaxial creep constitutive model by the well known Prandtl-Reuss equations as:

$$\dot{\varepsilon}_r^c = \frac{\dot{\varepsilon}_e^c}{\sigma_e}\big[\sigma_r - 0.5(\sigma_\theta + \sigma_z)\big] \quad (45)$$

$$\dot{\varepsilon}_\theta^c = \frac{\dot{\varepsilon}_e^c}{\sigma_e}\big[\sigma_\theta - 0.5(\sigma_r + \sigma_z)\big] \quad (46)$$

$$\dot{\varepsilon}_z^c = \frac{\dot{\varepsilon}_e^c}{\sigma_e}\big[\sigma_z - 0.5(\sigma_r + \sigma_\vartheta)\big] \quad (47)$$

where $\dot{\varepsilon}_e^c$ and σ_e are the effective creep strain rate and the effective stress respectively. Considering the case of plane strain ($\dot{\varepsilon}_z^c = 0$) and Norton's law (Eq. (8)), the radial and circumferential strain rates can be written as follows,

$$\dot{\varepsilon}_r^c = -\frac{3}{4} B(r) \sigma_e^{n_0 - 1} (\sigma_\theta - \sigma_r) \tag{48}$$

$$\dot{\varepsilon}_\theta^c = \frac{3}{4} B(r) \sigma_e^{n_0 - 1} (\sigma_\theta - \sigma_r) \tag{49}$$

Considering the Von Mises equivalent stress in the case of plane strain,

$$\sigma_e = \frac{\sqrt{3}}{2} (\sigma_\theta - \sigma_r) \tag{50}$$

Then Eqs. (48) and (49) may be rewritten as follows:

$$\dot{\varepsilon}_r^c = -\frac{\sqrt{3}}{2} B(r) \sigma_e^{n_0} \tag{51}$$

$$\dot{\varepsilon}_\theta^c = \frac{\sqrt{3}}{2} B(r) \sigma_e^{n_0} \tag{52}$$

Substituting Eqs. (51) and (52) into differential Eq. (44) the following differential equation is obtained,

$$r^2 \frac{d^2 \dot{u}}{dr^2} + (I\gamma + 1) r \frac{d\dot{u}}{dr} + (L\gamma - 1)\dot{u} = -\frac{\sqrt{3}}{2} \frac{(1-2\nu)}{(1-\nu)} I b_0 \left[(\gamma + b_1 + 2) r^{b_1 + 1} \sigma_e^{n_0} + r^{b_1 + 2} \frac{d\sigma_e^{n_0}}{dr} \right] \tag{53}$$

The general solution of the displacement $\dot{u}$ is,

$$\dot{u}(r) = D_1 r^{m_1} + D_2 r^{m_2} + u_1' r^{m_1} + u_2' r^{m_2} \tag{54}$$

where

$$u_1' = \int -\frac{r^{m_2} R'(r)}{w\left(r^{m_1}, r^{m_2}\right)} dr \tag{55}$$

$$u_2' = \int -\frac{r^{m_1} R'(r)}{w\left(r^{m_1}, r^{m_2}\right)} \tag{56}$$

$$w\left(r^{m_1}, r^{m_2}\right) = (m_2 - m_1) r^{m_1 + m_2 - 1} \tag{57}$$

$$R'(r) = -\frac{\sqrt{3}}{2} \frac{(1-2\nu)}{(1-\nu)} I b_0 \left[(\gamma + b_1 + 2) r^{b_1 + 1} \sigma_e^{n_0} + r^{b_1 + 2} \frac{d\sigma_e^{n_0}}{dr} \right] \tag{58}$$

The corresponding stress rates are,

$$\dot{\sigma}_r = \left(\bar{c}_{11}m_1 + \bar{c}_{12}\right)D_1 r^{\gamma+m_1-1} + \left(\bar{c}_{11}m_2 + \bar{c}_{12}\right)D_2 r^{\gamma+m_2-1} + \left(\bar{c}_{11}m_1 + \bar{c}_{12}\right)u_1{}' r^{\gamma+m_1-1}$$
$$+\left(\bar{c}_{11}m_2 + \bar{c}_{12}\right)u_2{}' r^{\gamma+m_2-1} + \bar{c}_{11}\left(\frac{\partial u_1{}'}{\partial r}\right)r^{\gamma+m_1} + \bar{c}_{11}\left(\frac{\partial u_2{}'}{\partial r}\right)r^{\gamma+m_2} + \frac{\sqrt{3}}{2}\bar{\lambda}_2 b_0 r^{\gamma+b_1}\sigma_e^{n_0} \tag{59}$$

$$\dot{\sigma}_\theta = \left(\bar{c}_{12}m_1 + \bar{c}_{12}\right)D_1 r^{\gamma+m_1-1} + \left(\bar{c}_{12}m_2 + \bar{c}_{11}\right)D_2 r^{\gamma+m_2-1} + \left(\bar{c}_{12}m_1 + \bar{c}_{11}\right)u_1{}' r^{\gamma+m_1-1}$$
$$+\left(\bar{c}_{12}m_2 + \bar{c}_{11}\right)u_2{}' r^{\gamma+m_2-1} + \bar{c}_{12}\left(\frac{\partial u_1{}'}{\partial r}\right)r^{\gamma+m_1} + \bar{c}_{12}\left(\frac{\partial u_2{}'}{\partial r}\right)r^{\gamma+m_2} - \frac{\sqrt{3}}{2}\bar{\lambda}_2 b_0 r^{\gamma+b_1}\sigma_e^{n_0} \tag{60}$$

To determine the unknown constants D_1 and D_2 in Eq. (54), boundary conditions have to be used. Since inside and outside pressures do not change with time, the boundary conditions for stress rates at the inner and outer surfaces may be written as:

$$\begin{cases} \dot{\sigma}_r = 0 \quad , \quad r = a \\ \dot{\sigma}_r = 0 \quad , \quad r = b \end{cases} \tag{61}$$

The unknown constants D_1 and D_2 are as follows:

$$D_1 = \left\{\left(\bar{c}_{11}m_1 + \bar{c}_{12}\right)\left(u_1{}'(b)a^{\gamma+m_2-1}b^{\gamma+m_1-1} - u_1{}'(a)a^{\gamma+m_1-1}b^{\gamma+m_2-1}\right) + \left(\bar{c}_{11}m_2 + \bar{c}_{12}\right)\right.$$
$$\left(u_2{}'(b)a^{\gamma+m_2-1}b^{\gamma+m_2-1} - u_2{}'(a)a^{\gamma+m_2-1}b^{\gamma+m_2-1}\right) + \bar{c}_{11}\left[\left(\frac{\partial u_1{}'}{\partial r}\right)_{r=b} a^{\gamma+m_2-1}b^{\gamma+m_1} - \left(\frac{\partial u_1{}'}{\partial r}\right)_{r=a} a^{\gamma+m_1}b^{\gamma+m_2-1}\right]$$
$$+\bar{c}_{11}\left[\left(\frac{\partial u_2{}'}{\partial r}\right)_{r=b} a^{\gamma+m_2-1}b^{\gamma+m_2} - \left(\frac{\partial u_2{}'}{\partial r}\right)_{r=a} a^{\gamma+m_2}b^{\gamma+m_2-1}\right] + \frac{\sqrt{3}}{2}\bar{\lambda}_2 b_0\left[\sigma_e^{n_0}(b)a^{\gamma+m_2-1}b^{\gamma+b_1}\,\sigma_e^{n_0}(b)a^{\gamma+b_1}b^{\gamma+m_2-1}\right]\Big\}$$
$$\Big/\left\{\left(\bar{c}_{11}m_1 + \bar{c}_{12}\right)\left(a^{\gamma+m_1-1}b^{\gamma+m_2-1} - a^{\gamma+m_2-1}b^{\gamma+m_1-1}\right)\right\} \tag{62}$$

$$D_2 = \left\{\left(\bar{c}_{11}m_2 + \bar{c}_{12}\right)\left(u_2{}'(b)a^{\gamma+m_1-1}b^{\gamma+m_2-1} - u_2{}'(a)a^{\gamma+m_2-1}b^{\gamma+m_1-1}\right) + \left(\bar{c}_{11}m_1 + \bar{c}_{12}\right)\right.$$
$$\left(u_1{}'(b)a^{\gamma+m_1-1}b^{\gamma+m_1-1} - u_1{}'(a)a^{\gamma+m_1-1}b^{\gamma+m_1-1}\right) + \bar{c}_{11}\left[\left(\frac{\partial u_2{}'}{\partial r}\right)_{r=b} a^{\gamma+m_1-1}b^{\gamma+m_2} - \left(\frac{\partial u_2{}'}{\partial r}\right)_{r=a} a^{\gamma+m_2}b^{\gamma+m_1-1}\right]$$
$$+\bar{c}_{11}\left[\left(\frac{\partial u_1{}'}{\partial r}\right)_{r=b} a^{\gamma+m_1-1}b^{\gamma+m_1} - \left(\frac{\partial u_1{}'}{\partial r}\right)_{r=a} a^{\gamma+m_1}b^{\gamma+m_1-1}\right] + \frac{\sqrt{3}}{2}\bar{\lambda}_2 b_0\left[\sigma_e^{n_0}(b)a^{\gamma+m_1-1}b^{\gamma+b_1}\,\sigma_e^{n_0}(b)a^{\gamma+b_1}b^{\gamma+m_1-1}\right]\Big\}$$
$$\Big/\left\{\left(\bar{c}_{11}m_2 + \bar{c}_{12}\right)\left(a^{\gamma+m_2-1}b^{\gamma+m_1-1} - a^{\gamma+m_1-1}b^{\gamma+m_2-1}\right)\right\} \tag{63}$$

when the stress rate is known, the calculation of stresses at any time t_i should be performed iteratively.

$$\sigma_{ij}^{(i)}(r,t_i) = \sigma_{ij}^{(i-1)}(r,t_{i-1}) + \dot{\sigma}_{ij}^{(i)}(r,t_i)dt^{(i)} \tag{64}$$

where

$$t_i = \sum_{k=0}^{i} dt^{(k)} \tag{65}$$

5 NUMERICAL RESULTS AND DISCUSSION

In the previous sections, the analytical solution of creep stresses for FGM thick-walled cylindrical vessels subjected to uniform pressures on the inner and outer surfaces and uniform magnetic field were obtained. In this section, some profiles are plotted for the radial stress, circumferential stress, effective stress, radial stress rate and circumferential stress rate as a function of radial direction for different times after creep. An FGM thick-walled cylindrical vessel with creep behavior under internal and external pressure and uniform magnetic field is considered. Mechanical properties of the cylinder, such as modulus of elasticity, density, thermal expansion coefficient, moisture concentration coefficient, thermal conductivity, moisture diffusivity coefficient and magnetic permeability are assumed to obey the power-law variation. In-homogeneity constants γ range from -2 to $+2$. The following data for loading and material properties are used in this investigation.

$$b/a = 2 \;,\; E_0 = 22GPa \;,\; \nu = 0.33 \;,\; \alpha_0 = 1.2\times10^{-6}K^{-1} \;,\; \beta_0 = 0.8\times10^{-4}\, m^3/kg \;,\; \rho_0 = 7860\, kg/m^3$$

$$\mu_0 = 4\pi\times10^{-7}\, H/m \;,\; H_z = 223\times10^{9}\, A/m \;,\; T_i = 200^{\circ}C \;,\; T_0 = 25^{\circ}C \;,\; M_i = 0 \;,\; M_0 = 3$$

$$P_i = 80MPa \;,\; P_0 = 0MPa \;,\; \omega = 1000\, rad/s \;,\; b_0 = 0.11\times10^{-36} \;,\; b_1 = -5 \;,\; n_0 = 3$$

The distributions of creep stress components σ_r and σ_θ and effective stress σ_e at zero time for values of $\gamma = \pm1,\ \pm2$, are plotted in Figs. 1,2,3, respectively. It can be seen from Fig. 1 that the boundary conditions for radial stress at the inner and outer surfaces of the cylinder are satisfied for all material properties. As this figure shows maximum values of radial stress belong to $\gamma = -2$ and the minimum values belong to $\gamma = 2$. According to Fig. 2 and Fig. 3, circumferential and effective stresses for $\gamma = 2,1,-1$ is tensile throughout thickness while for $\gamma = -2$ is compressive. The absolute maximums of radial and circumferential stresses for $\gamma = -2,-1,1$ occur at the inner edge, which means the maximum shear stress for $\gamma = -2,-1,1$ which is $\tau_{\max} = (\sigma_\theta - \sigma_r)/2$ will be very high on the inner surface of the vessel and can cause yielding to occur.

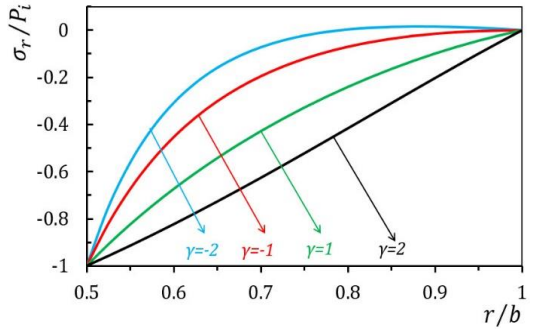

Fig.1
Normalized radial stress versus dimensionless radius at zero time.

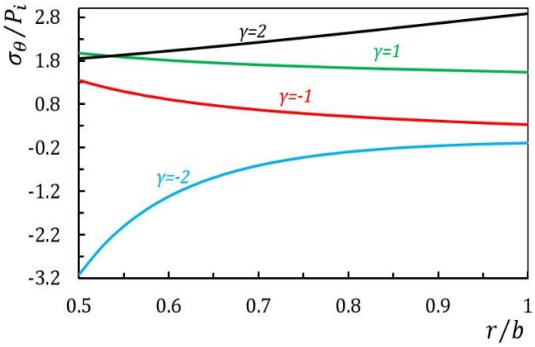

Fig.2
Normalized circumferential stress versus dimensionless radius at zero time.

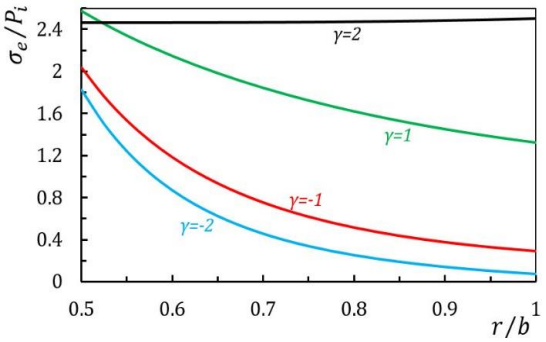

Fig.3
Normalized effective stress versus dimensionless radius at zero time.

Radial and circumferential stress rates redistributions for different values of γ, are shown in Figs. 4 and 5. Fig. 4 shows that the radial stress rates for all values of γ, are zero at the inner and outer surfaces of the cylinder which satisfy the boundary conditions. The maximum rate of change of radial stresses belongs to $\gamma = -2$ and the minimum rate belongs to $\gamma = 2$. Therefore minimum changes in radial stresses with time will take place for the material identified by $\gamma = 2$ as will be explained next in radial stress redistributions. It can be seen from Fig. 5 that, at the inner radius of the cylinder the circumferential stress rates increases as γ decreases.

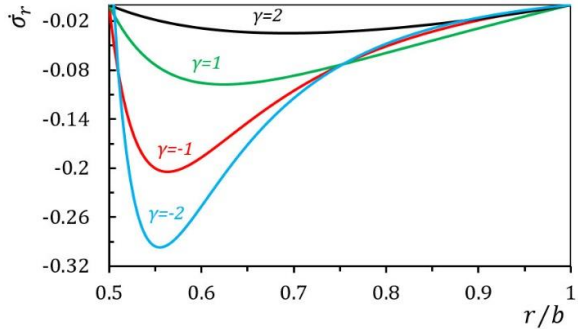

Fig.4
Radial stress rate versus dimensionless radius at zero time.

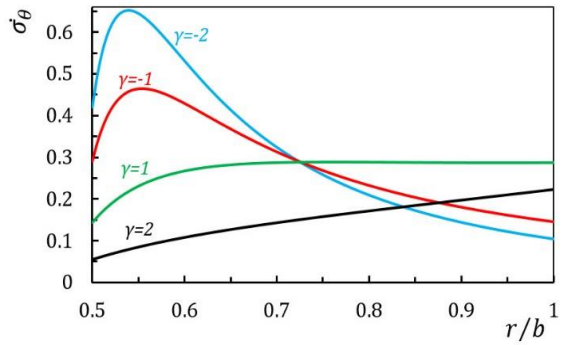

Fig.5
Circumferential stress rate versus dimensionless radius at zero time.

Time-dependent creep stress redistributions for $\gamma = 2$ are shown in Figs. 6-8. Fig. 6 shows the time-dependent radial stress from initial elastic at zero time to fourth selected time interval. There is an increase in the value of the radial stress as time increases. It also satisfies the boundary conditions at the inner and outer surfaces of the cylinder. Circumferential stress redistribution for this case $\gamma = 2$ from initial elastic at zero time to fourth selected time interval is shown in Fig. 7. It is clear that the value of the circumferential stress increases as time increases. The effective stress along the radius is plotted in Fig. 8. It can be seen that the value of the circumferential stress increases as time increases and also the maximum change in the value of effective stress occur at the outer surface of the cylinder. It is noted that the maximum shear stress at the inner and outer surfaces of the vessel is increasing with time.

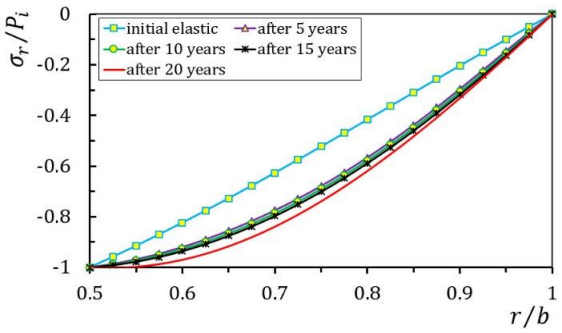

Fig.6
Normalized radial creep stress redistribution from initial elastic at zero time to fourth selected time interval for the case $\gamma = 2$.

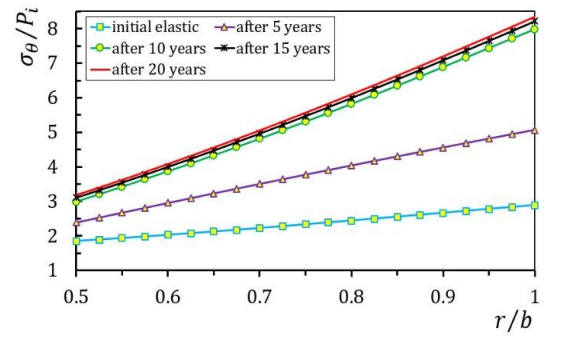

Fig.7
Normalized circumferential creep stress redistribution from initial elastic at zero time to fourth selected time interval for the case $\gamma = 2$.

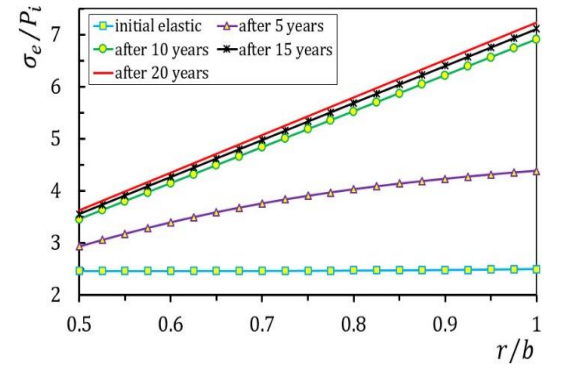

Fig.8
Normalized effective creep stress redistribution from initial elastic at zero time to fourth selected time interval for the case $\gamma = 2$.

Figs. 9 and 10 show the radial and circumferential stress rates along the thickness of FGM cylinder, from initial elastic at zero time to fourth selected time interval for the case $\gamma = 2$. It can be seen from Figs. 9 and 10 that the rates of the radial and circumferential stress decreases as time increases.

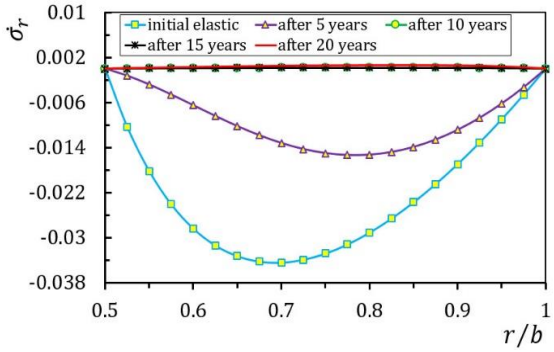

Fig.9
Radial stress rate redistribution from initial elastic at zero time to fourth selected time interval for the case $\gamma = 2$.

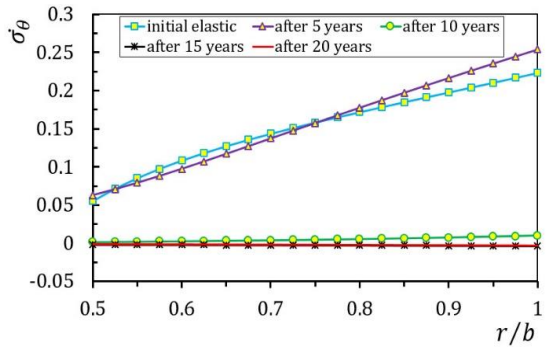

Fig.10
Circumferential stress rate redistribution from initial elastic at zero time to fourth selected time interval for the case $\gamma = 2$.

Figs. 11-13 show the effects of adding internal pressure, angular velocity and inner surface temperature on effective stress for the case $\gamma = 2$ after 20 years from creep. It can be seen from these figures that effective stress increases as internal pressure and angular velocity increase and inner surface temperature decreases. It must be noted that in these figures the external pressure is $P_0 = 0MPa$ and outer surface temperature is $T_0 = 25^\circ C$.

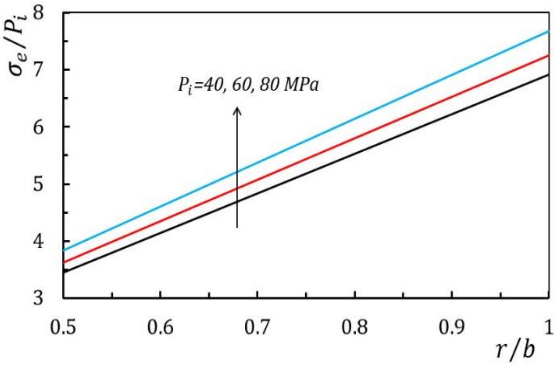

Fig.11
The effect of adding internal pressure on effective stress for the case $\gamma = 2$ after 20 years from creep.

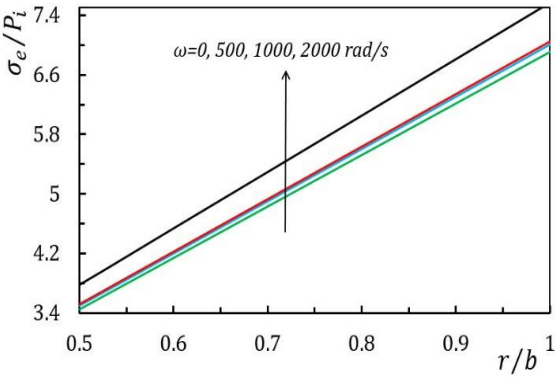

Fig.12
The effect of adding angular velocity on effective stress for the case $\gamma = 2$ after 20 years from creep.

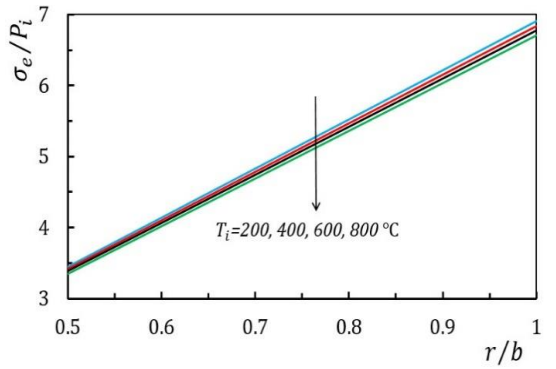

Fig.13
The effect of adding inner surface temperature on effective stress for the case $\gamma = 2$ after 20 years from creep.

Temperature and moisture distributions of four different values of γ is shown in Figs. 14 and 15.

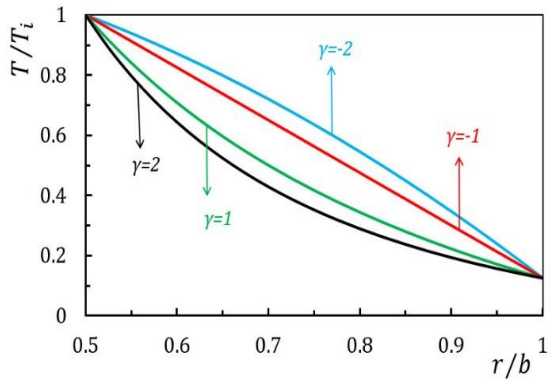

Fig.14
Normalized temperature distribution of FGM thick walled cylindrical vessel for values of $\gamma = \pm 1,\ \pm 2$.

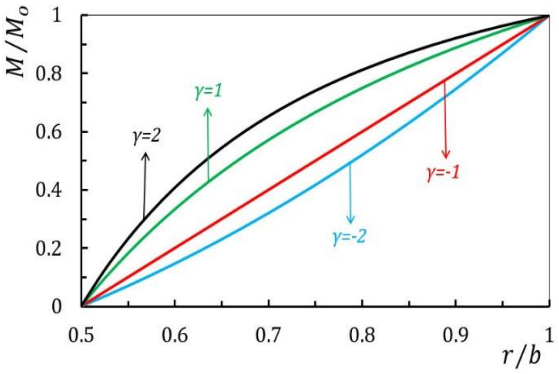

Fig.15
Normalized moisture distribution of FGM thick walled cylindrical vessel for values of $\gamma = \pm 1,\ \pm 2$.

6 CONCLUSIONS

In this article, assuming that the thermo-creep response of the material is governed by Norton's law, an analytical solution is presented for the calculation of stresses of FGM thick-walled cylindrical pressure vessels. For the stress analysis in a cylinder, having material creep behavior, the solutions of the stresses at a time equal to zero (i.e. the initial stress state) are needed, which corresponds to the solution of materials with linear magnetohygrothermoelastic behavior. The analytical solution is obtained for the condition of plane strain. It is assumed that the material properties change as graded in radial direction to a power law function. To show the effect of inhomogeneity on the stress distributions, different values are considered for in-homogeneity constants. The governing coupled differential equations are exactly solved. The cylinder is subjected to internal and external pressure and uniform magnetic field. The temperature and moisture concentration distributions are obtained separately in an uncoupled hygrothermal analysis by solving heat conduction and moisture diffusion equations. For the stress analysis after creeping for a long time, the iterative procedure is necessary. It could be seen that the in-homogeneity constants have significant influence on the distributions of the creep stresses. The best materials is identified by $\gamma = -1, -2$ in which the minimum shear stress distribution will occur throughout the thickness of the FGM cylinder.

REFERENCES

[1] Xie H., Dai H. L., Rao Y. N., 2013, Thermoelastic dynamic behaviors of a FGM hollow cylinder under non-axisymmetric thermo-mechanical loads, *Journal of Mechanics* **29**: 109-120.

[2] Levyakov S. V., Kuznetsov V. V., 2014, Nonlinear stability analysis of functionally graded shells using the invariant-based triangular finite element, *Journal of Applied Mathematics and Mechanics* **94**: 101-117.

[3] Nejad, M. Z. Fatehi, P. 2015, Exact elasto-plastic analysis of rotating thick-walled cylindrical pressure vessels made of functionally graded materials, *International Journal of Engineering Science* **86**, 26–43.

[4] Nejad, M. Z., Jabbari, M. Ghannad, M. 2015a, Elastic analysis of FGM rotating thick truncated conical shells with axially-varying properties under non-uniform pressure loading, *Composite Structures* **122**, 561–569.
[5] Nejad, M. Z., Jabbari, M. Ghannad, M. 2015b, Elastic analysis of rotating thick cylindrical pressure vessels under non-uniform pressure: Linear and non-linear thickness, *Periodica Polytechnica- Mechanical Engineering* **59**, 65–73.
[6] Nejad, M. Z., Jabbari, M. Ghannad, M. 2017, A general disk form formulation for thermo-elastic analysis of functionally graded thick shells of revolution with arbitrary curvature and variable thickness, *Acta Mechanica* **228**, 215–231.
[7] Nejad, M. Z., Rastgoo, A. Hadi, A., 2014, Exact elasto-plastic analysis of rotating disks made of functionally graded materials," *International Journal of Engineering Sciences*, **85**, 47–57.
[8] Nejad M. Z., Jabbari M., Ghannad M., 2015c, Elastic analysis of axially functionally graded rotating thick cylinder with variable thickness under non-uniform arbitrarily pressure loading, *International Journal of Engineering Science* **89**: 86-99.
[9] Nejad M. Z., Jabbari M., Ghannad M., 2015d, Thermo-elastic analysis of axially functionally graded rotating thick cylindrical pressure vessels with variable thickness under mechanical loading, *International Journal of Engineering Science* **96**: 1-18.
[10] Jabbari, M., Nejad, M. Z., Ghannad, M. 2016a, Effect of thickness profile and FG function on rotating disks under thermal and mechanical loading, *Journal of Mechanics* **32**, 35–46.
[11] Jabbari, M., Nejad, M. Z., Ghannad, M. 2016b, Thermo-elastic analysis of axially functionally graded rotating thick truncated conical shells with varying thickness, *Composites Part B- Engineering* **96**, 20–34.
[12] Attia Y. G., Fitzgeorge D., Pope J. A., 1954, An experimental investigation of residual stresses in hollow cylinders due to the creep produced by thermal stresses, *Journal of the Mechanics and Physics of Solids* **2**: 238-258.
[13] Weir C. D., 1957, The creep of thick walled tube under internal pressure, *Journal of Applied Mechanics* **24**: 464-466.
[14] Wah T., 1961, Creep collapse of cylindrical shells, *Journal of the Franklin Institute* **272**: 45-60.
[15] Bhatnagar N. S., Gupta S. K., 1969, Analysis of thick-walled orthotropic cylinder in the theory of creep, *Journal of the Physical Society of Japan* **27**: 1655-1662.
[16] Besseling J. F., 1962, *Investigation of Transient Creep in Thick-Walled Tubes Under Axially Symmetric Loading*, Springer-Verlag OHG.
[17] Pai D. H., 1967, Steady-state creep analysis of thick-walled orthotropic cylinders, *International Journal of Mechanical Sciences* **9**: 335-348.
[18] Sankaranarayanan R., 1969, Steady creep of circular cylindrical shells under combined lateral and axial pressures, *International Journal of Solids and Structures* **5**: 17-32.
[19] Murakami S., Iwatsuki S.h., 1969, Transient creep of circular cylindrical shells, *International Journal of Mechanical Sciences* **11**: 897-912.
[20] Murakami S., Suzuki K., 1971, On the creep analysis of pressurized circular cylindrical shells, *International Journal of Non-Linear Mechanics* **6**: 377-392.
[21] Sim R. G., Penny R. K., 1971, Plane strain creep behaviour of thick-walled cylinders, *International Journal of Mechanical Sciences* **12**: 987-1009.
[22] Murakami S., Iwatsuki S.h., 1971, Steady-state creep of circular cylindrical shells, *Bulletin of the JSME* **73**: 615-623.
[23] Kashkoli M. D., Nejad M. Z., 2014, Effect of heat flux on creep stresses of thick-walled cylindrical pressure vessels, *Journal of Applied Research and Technology* **12**: 585-597.
[24] Bhatnagar N. S., Arya V. K., 1974, Large strain creep analysis of thick-walled cylinders, *International Journal of Non-Linear Mechanics* **9**:127-140.
[25] Murakami S., Tanaka E., 1976, On the creep buckling of circular cylindrical shells, *International Journal of Mechanical Sciences* **18**: 185-194.
[26] Jones N., Sullivan P. F., 1976, On the creep buckling of a long cylindrical shell, *International Journal of Mechanical Sciences* **18**: 209-213.
[27] Arya V. K., Debnath K. K., Bhatnagar N. S., 1983, Creep analysis of orthotropic circular cylindrical shells, *International Journal of Pressure Vessels and Piping* **11**:167-190.
[28] Loghman A., Wahab M. A., 1996, Creep damage simulation of thick-walled tubes using the theta projection concept, *International Journal of Pressure Vessels and Piping* **67**: 105-111.
[29] Yang Y. Y., 2000, Time-dependent stress analysis in functionally graded materials, *International Journal of Solids and Structures* **37**: 7593-7608.
[30] Gupta S. K., Pathak S., 2001, Thermo creep transition in a thick walled circular cylinder under internal pressure, *Indian Journal of Pure and Applied Mathematics* **32**: 237-253.
[31] Jahed H., Bidabadi J., 2003, An axisymmetric method of creep analysis for primary and secondary creep, *International Journal of Pressure Vessels and Piping* **80**: 597-606.
[32] Chen J. J., Tu Sh. T., Xuan F. Z., Wang Z. D., 2007, Creep analysis for a functionally graded cylinder subjected to internal and external pressure, *The Journal of Strain Analysis for Engineering Design* **42**: 69-77.
[33] You L. H., Ou H., Zheng Z. Y., 2007, Creep deformations and stresses in thick-walled cylindrical vessels of functionally graded materials subjected to internal pressure, *Composite Structures* **78**: 285-291.
[34] Altenbach H., Gorash Y., Naumenko K., 2008, Steady-state creep of a pressurized thick cylinder in both the linear and the power law ranges, *Acta Mechanica* **195**: 263-274.

[35] Singh T., Gupta V. K., 2009a, Creep analysis of an internally pressurized thick cylinder made of a functionally graded composite, *Journal of Strain Analysis* **44**: 583-594.
[36] Singh T., Gupta V. K., 2009b, Effect of material parameters on steady state creep in a thick composite cylinder subjected to internal pressure, *The Journal of Engineering Research* **6**: 20-32.
[37] Singh T., Gupta V. K., 2010a, Modeling of creep in a thick composite cylinder subjected to internal and external pressures, *International Journal of Materials Research* **2**: 279-286.
[38] Singh T., Gupta V. K., 2010b, Modeling steady state creep in functionally graded thick cylinder subjected to internal pressure, *Journal of Composite Materials* **44**: 1317-1333.
[39] Nejad M. Z., Kashkoli M. D., 2014, Time-dependent thermo-creep analysis of rotating FGM thick-walled cylindrical pressure vessels under heat flux, *International Journal of Engineering Science* **82**: 222-237.
[40] Loghman A., Ghorbanpour Arani A., Amir A. S., Vajedi A., 2010, Magnetothermoelastic creep analysis of functionally graded cylinders, *International Journal of Pressure Vessels and Piping* **87**: 389-395.
[41] Singh T., Gupta V. K., 2011, Effect of anisotropy on steady state creep in functionally graded cylinder, *Composite Structures* **93**: 747-758.
[42] Kashkoli M. D., Nejad M. Z., 2015, Time-dependent thermo-elastic creep analysis of thick-walled spherical pressure vessels made of functionally graded materials, *Journal of Theoretical and Applied Mechanics* **53**:1053-1065.
[43] Dai H. L., Zheng H. Y., 2012, Creep buckling and post-buckling analyses of a viscoelastic FGM cylindrical shell with initial deflection subjected to a uniform in-plane load, *Journal of Mechanics* **28**: 391-399.
[44] Sharma S., Sahay I., Kumar R., 2012, Creep transition in non homogeneous thick-walled circular cylinder under internal and external pressure, *Applied Mathematical Sciences* **122**: 6075-6080.
[45] Jamian S., Sato H., Tsukamoto H., Watanabe Y., 2013, Creep analysis of functionally graded material thick-walled cylinder, *Applied Mechanics and Materials* **315**: 867-871.
[46] Singh T., Gupta V. K., 2014, Analysis of steady state creep in whisker reinforced functionally graded thick cylinder subjected to internal pressure by considering residual stress, *Mechanics of Advanced Materials and Structures* **21**: 384-392.
[47] Nejad M. Z., Hoseini Z., Niknejad A., Ghannad M., 2015, Steady-state creep deformations and stresses in FGM rotating thick cylindrical pressure vessels, *Journal of Mechanics* **31**: 1-6.
[48] Kashkoli M. D., Tahan K. N., Nejad M. Z., 2017, Time-dependent thermomechanical creep behavior of FGM thick hollow cylindrical shells under non-uniform internal pressure, *International Journal of Applied Mechanics* **9**: 750086.
[49] Kashkoli M. D., Tahan K. N., Nejad M. Z., 2017, Time-dependent creep analysis for life assessment of cylindrical vessels using first order shear deformation theory, *Journal of Mechanics* **33**: 461-474.
[50] Sharma S., Yadav S., Sharma R., 2017, Thermal creep analysis of functionally graded thick-walled cylinder subjected to torsion and internal and external pressure, *Journal of Solid Mechanics* **9**: 302-318.
[51] Loghman A., Shayestemoghadam H., Loghman S., 2016, Creep evolution analysis of composite cylinder made of polypropylene reinforced by functionally graded MWCNTs, *Journal of Solid Mechanics* **8**: 372-383.
[52] Loghman A., Atabakhshian V., 2012, Semi-analytical solution for time-dependent creep analysis of rotating cylinders made of anisotropic exponentially graded material (EGM), *Journal of Solid Mechanics* **4**: 313-326.
[53] Ghorbanpour Arani A., Kolahchi R., Mosallaie Barzoki A. A., Loghman A., 2011, Time-dependent thermo-electro-mechanical creep behavior of radially polarized FGPM rotating cylinder, *Journal of Solid Mechanics* **3**: 142-157.
[54] Aleayoub S. M. A., Loghman A., 2010, Creep stress redistribution analysis of thick-walled FGM spheres, *Journal of Solid Mechanics* **2:** 115-128.